Available online at www.sciencedirect.com
SCIENCE DIRECT®
Polymer 45 (2004) 2587–2601
polymer
www.elsevier.com/locate/polymer

Phase morphology and stability of co-continuous (PPE/PS)/PA6 and PS/PA6 blends: effect of rheology and reactive compatibilization

R.T. Tol[a], G. Groeninckx[a,*], I. Vinckier[b], P. Moldenaers[b], J. Mewis[b]

[a]*Laboratory for Macromolecular Structural Chemistry, Department of Chemistry, Katholieke Universiteit Leuven (KU Leuven), Celestijnenlaan 200F, B-3001 Heverlee, Belgium*

[b]*Department of Chemical Engineering, Catholic University of Leuven, de Croylaan 46, B-3001 Heverlee, Belgium*

Received 19 September 2003; received in revised form 16 December 2003; accepted 17 December 2003

Abstract

(PPE/PS)/PA6 and PS/PA6 blends were prepared by means of melt-extrusion. They were compatibilized using the reactive styrene-maleic anhydride copolymer with 2 wt% maleic anhydride (SMA2). The effect of compatibilization on the phase inversion and the stability of the resulting co-continuous blend structures were investigated using scanning electron microscopy, dissolution and extraction experiments. The onset of co-continuity shifted towards lower PA6 concentrations according to the change in blend viscosity ratio. The melting order of the components inside the extruder could result in a change in the observed co-continuity interval in slowly developing phase morphologies. The unmodified co-continuous blends were not stable and did break-up into a droplet/matrix type of morphology upon annealing in the melt depending on the blend composition. Although the stability of the threads during annealing improved upon compatibilization because of the lower resulting interfacial tension, the decreased possibility for recombination and coalescence during flow reduced the co-continuous region for the compatibilized blends. It is proposed that a dynamic equilibrium between break-up and recombination phenomena after the initial network formation is necessary to maintain the network structure.

Keywords: Co-continuity; Reactive compatibilization; Melt-stability

1. Introduction

Immiscible polymer blends can reveal a wide range of microstructures. At low volume fractions of one of the blend components the minor component will be dispersed into the matrix of the major component. At higher volume fractions a co-continuous structure can be generated, which consists of strongly interpenetrating domains of both blend components. In such co-continuous structures each of the blend components can fully contribute to the final properties. With respect to their properties, a thorough understanding of both the formation of these interconnected structures during processing as well as their stability in the melt-state is crucial.

The formation of co-continuous network structures was long believed to be only possible in a narrow composition range around the phase inversion concentration. It was attempted to predict the point where phase inversion occurs by relating it to the viscosity ratio of the two blend components, hereby accounting for the tendency of the lower viscous component to encapsulate the component with a higher viscosity [1–8]. More recent investigations, however, have shown that the phase inversion is not depending on the viscosity ratio alone and that in fact co-continuous morphologies can be obtained over a wide range of volume fractions, the so-called co-continuity interval [9–20].

It has been demonstrated that this co-continuity interval is clearly affected by the interfacial tension of the blend [9–11], by the processing conditions such as mixing time and type of flow [9,12,13,20] and by the rheological characteristics of the blend components [9]. Also, modified theories for phase inversion were proposed in which the effect of elasticity of the blend components, i.e. the tendency of the more elastic component to encapsulate the less elastic component, is accounted for [16,17,21,22]. Such studies are based the work of van Oene [23], who proposed a

* Corresponding author. Tel.: +32-16-327440; fax: +32-16-327990.
E-mail address: gabriel.groeninckx@chem.kuleuven.ac.be (G. Groeninckx).

0032-3861/$ - see front matter © 2004 Elsevier Ltd. All rights reserved.
doi:10.1016/j.polymer.2003.12.072

relation for the elastic contribution to the effective interfacial tension under dynamic conditions.

Scott and Macosko [24] showed that the phase morphology development of immiscible polymer blends in the initial melting stages in a batch mixer could be described by a sheeting mechanism whereby sheets are pulled off the softening pellets. Sundararaj et al. [25] showed that this sheeting mechanism occurs in single screw as well as in twin-screw extrusion. Assuming initial sheeting formation, Willemse et al. [9] proposed a semi-empirical relation using geometrical considerations for the formation of a co-continuous network. It provides upper and lower concentration limits for co-continuity as a function of the viscosity ratio, the interfacial tension and the shear rate. In these investigations, the stability of the network obtained after the initial sheeting process was considered as the determining factor for the resulting type of morphology (droplet/matrix or co-continuous).

Luciani et al. [26] also indicated the importance of the stability of the fibrillar structure, but suggested a coalescence mechanism of threads during processing to explain the presence of both nodular and fibrillar structures close to the phase inversion region. Li et al. [27] recently proposed a general mechanism for the formation of co-continuity based on thread lifetime versus droplet lifetime during processing for different types of blend interfaces. A thread/thread coalescence phenomenon is proposed for the formation of the network when the interfacial tension of the blend is low. In this case, the thread lifetime is expected to be higher than the droplet lifetime. In case of a high interfacial tension blend, the droplet lifetime is higher than the thread lifetime resulting in a droplet-droplet coalescence mechanism for obtaining a network structure. It was shown that the formation mechanism has profound consequences on the resulting blend microstructure.

The instability of the co-continuous structures is one of the main problems when trying to apply these morphologies. The interfacial tension will drive the system towards a smaller interfacial area, resulting in break-up, retraction or strong coarsening of elongated structures. During annealing of a co-continuous blend in the molten state, a droplet/matrix morphology or a much coarser co-continuous morphology is generated and the region for co-continuity becomes narrower [11,14,15,28–31]. A possible route for stabilizing the co-continuous phase network structure could be the addition of a compatibilizer, which decreases the interfacial tension. A number of authors have demonstrated that the stability of an elongated thread in quiescent conditions can be enhanced significantly as a result of the lower interfacial tension [32,33]. Indeed, Verhoogt et al. [14] demonstrated that immiscible blends with a low interfacial tension display a wide region of co-continuity. Veenstra et al. [11] reported a similar result for homopolymer/copolymer blends. Other authors, however, observed that in blends where a compatibilizer was added, the composition interval in which co-continuity occurred was narrowed down and the percolation phenomena shifted towards higher concentrations [14,15,18,20,22,34].

In this investigation the morphology development in blends of PS/PA6 and (PPE/PS)/PA6 will be studied. Compatibilization of these blends is realized by adding a reactive compatibilizer SMA2 as a third component to the two model blends, using reactive extrusion. An attempt will be made to elucidate the source of the contradictory observations on compatibilized co-continuous blends by separating the effects of flow during extrusion (where the network is formed) from the network stability under quiescent conditions. This implies a thorough determination of the blend composition region for co-continuity and a subsequent investigation of the melt-stability of the thus formed structures under quiescent conditions. The great advantage of using the present blend systems is that their viscosity and elasticity ratios can be changed by adjusting the ratio of PPE versus PS, without altering the interfacial tension of the blend [35].

2. Materials and methods

2.1. Materials

The polymers used in this study are listed in Table 1, together with their M_w and T_g Polyamide-6 (PA Akulon k123) was provided by DSM-Research. Atactic polystyrene (PS Styron E680) was supplied by DOW Benelux. The miscible polystyrene/polyphenylene-ether (PPE/PS) 50/50 (wt/wt) mixture was prepared by mixing PPE (supplied by GE Plastics) and PS (supplied by DOW) in a Haake Rheocord 90 twin-screw extruder [35]. Styrene-maleic anhydride copolymer SMA2 was provided by Bayer. PS and (PPE/PS) 50/50 (wt/wt) are miscible with SMA2 over the whole composition range [36,37]. The number after SMA denotes the wt% maleic anhydride in SMA.

2.2. Blend preparation

The blends were prepared on a co-rotating twin-screw mini-extruder designed by DSM-Research. Before processing, all materials were dried overnight under vacuum at 80 °C. Two different mixing procedures were applied. In mixing method 1, PS or (PPE/PS) were first premixed with SMA2, after which the pelletized material was mixed with PA6. In mixing method 2, SMA2 was premixed with PA6

Table 1
Molecular characteristics of the blend components used

Materials	M_w (g/mol)	T_g (°C)
PS	190,000	102
PPE/PS (50/50 wt/wt)	54,300/190,000	150
PA6	24,000	50
SMA2	120,000	105

and then blended with PS or (PPE/PS). From these mixing experiments the blending conditions that achieved the most optimal compatibilization results (strongest particle size decrease) could be deduced. A summary of the blending conditions is given in Table 2. During melt-blending the mixing chamber was saturated with N_2 gas to avoid oxidative degradation. After mixing, the blends were quenched in a mixture of CO_2/isopropanol (−78 °C) in order to freeze in the existing phase morphology.

2.3. Morphological characterization via dissolution experiments and quantitative extraction

The morphology of the extruded blends was analyzed by means of dissolution experiments. In this manner it could be determined whether the extruded blends were co-continuous or not. A small piece of the sample (about 0.025 cm^3) was immersed in formic acid at room temperature. Formic acid is a solvent for PA6 and a non-solvent for PS, (PPE/PS) and SMA2. A second piece was put in chloroform at room temperature. Chloroform is a solvent for PS, (PPE/PS) and SMA2 and a non-solvent for PA6. The complete procedure was repeated twice. With a droplet/matrix morphology, a solvent dissolving the matrix would cause disintegration of the sample, resulting in a milky suspension. In a co-continuous system, neither of the solvents could cause a complete disintegration of the blend.

Extraction tests were performed to obtain more information on the real 3D structure of the co-continuous network. For the extraction tests, about 1 cm of the extruded strands (about 0.05 cm^3) was put in formic acid for 14 days at room temperature to extract the PA6 phase. The weight of the strand before and after extraction was measured to determine the weight of PA6 that could be dissolved. Three samples were examined for every blend. The percentage of co-continuity of the PA6 phase was then determined by the ratio of the weight of PA6 dissolved over the total weight of PA6 added to the blend.

In general, the percolation threshold is defined as the concentration of the dispersed phase at which co-continuity sets in and a phase network starts to form. A further increase in this concentration will cause more material to be incorporated into the network, until finally a fully co-continuous phase network is formed. In this case, 100% of that component can be extracted by selective dissolution because all the material is interconnected. In practice, however, fully co-continuous phase networks are seldom encountered. There is always a degree of ambiguity in the determination of the width of the co-continuity interval. In this investigation, the co-continuity interval has been determined on the basis of the disintegration data; the blends that did not disintegrate in the dissolution tests were considered as co-continuous. The percentage of co-continuity was then estimated from the extraction data.

Table 2
Summary of the different blending conditions used

Extrusion procedure	Screw speed (rpm)	Temperature (°C)	Mixing time (min)
Method no. 1			
Step 1	100	260	8
Step 2	100	260	8
Method no. 2			
Step 1	100	240	4
Step 2	100	260	8

2.4. SEM microscopy

The phase morphology of the blends has also been characterized by scanning electron microscopy (SEM) on a Philips XL20. An extruded polymer strand was first broken in liquid nitrogen so that a fracture surface perpendicular to the extrusion direction was obtained. A Leica Ultracut UCT cryo-microtome at −100 °C was used to smooth the fractured surface. Images parallel to the direction of the flow were prepared in a similar fashion. Subsequently, the samples were etched in either formic acid or chloroform (16 and 40 h, respectively) to remove the dispersed phase. The etched surface was dried under vacuum and then coated with a conductive gold layer before SEM analysis.

The SEM photographs used for image analysis (see Section 2.5) were obtained after subjecting the samples to a thermal program typically used in dynamic crystallization experiments with DSC. This thermal treatment consisted of heating the sample at a rate of 10 °C/min to 260 °C, i.e. about 40 °C above the melting temperature of PA6. After an isothermal period of 3 min the blend sample was cooled at 10 °C/min to room temperature again. This procedure was followed to be able to compare later the morphological data with the results from DSC experiments.

2.5. Image analysis

Image analysis on the obtained SEM micrographs was performed using Leica Qwin image analysis software. The morphological parameters of the blends were quantified as follows. For the systems with a droplet/matrix structure, the average size and the size distribution of the dispersed particles were determined. About six SEM photographs (each containing about 150 particles) were analyzed for each blend. The number average particle diameter (D_n), volume average diameter (D_v) and the polydispersity (P) were calculated from:

$$D_n = \frac{\sum_i n_i d_i}{\sum_i n_i}$$

$$D_v = \frac{\sum_i n_i d_i^4}{\sum_i n_i d_i^3}$$

Polydispersity $P = D_v/D_n$

with n_i as the number of particles having diameter d_i.

The characteristic diameters are given as seen in SEM and were not corrected for the fact that not all particles were cut at their largest cross-section.

2.6. Rheometry

The pure polymers were characterized rheologically by means of dynamic rheological measurements A stress controlled rheometer from Rheometric Scientific (DSR200) was used for this purpose, equipped with a parallel plate geometry. Samples with a diameter of 25 mm and a thickness of 2 mm were compression moulded from the test material using a Carver press at a temperature of 240 °C. These disks were dried at 80 °C under vacuum prior to the measurements. The latter were performed at 260 °C under nitrogen atmosphere. The frequency was varied from 100 to 0.1 rad/s and the amplitude was kept small enough to ensure a linear viscoelastic response of the polymers.

3. Results and discussion

3.1. Rheological properties of the blend components

The morphology of an immiscible polymer blend is closely related to its rheology. Therefore, the rheological properties of the blend components have been studied here (see Figs. 1 and 2). The (PPE/PS) 50/50 mixture is found to be much more viscous and elastic than pure PS. The data also indicate that the viscosities of PS and (PPE/PS) 50/50 are hardly affected by adding small amounts of miscible SMA2 compatibilizer.

When adding SMA2 compatibilizer to PA6, the rheological properties of PA6 change quite significantly. During blending of the PA6 with SMA2 the melt viscosity of PA6 strongly increases as a result of the graft formation reaction between the PA6 amino-end groups and the SMA2 anhydride groups. The magnitude of the complex viscosity at 100 rad/s for a mixture of PA6 and SMA2 in a weight ratio of 65/35, is a decade larger than that of pure PA6 (see Fig. 1). Furthermore, the viscosity does not reach a plateau value at low frequencies. This suggests a network structure, which is confirmed by the data for the storage moduli G', which tends to reach a plateau value at low frequencies (Fig. 2), a characteristic of solid or gel-like structure. In addition, the PA6/SMA2 65/35 (wt/wt) sample was found not to dissolve in formic acid, it only swelled. Other authors reported similar results when high amounts of SMA2 compatibilizer were blended with PA6 or PA6,6 [38,39]. When the concentration of anhydride groups is much higher than the number of available amino-end groups of PA6 hydrolysis of the PA-amide groups results in PA chain scission and new carboxylic acid and amine groups; these then react with the excess anhydride groups of SMA [39]. Two possible factors thus can be proposed for the observed rheological behavior of PA6/SMA mixtures. First, the heterogeneity of the blend morphology can lead to an interface contribution to the storage modulus caused by the relaxation of the immiscible SMA domains during flow. Second, the elasticity can be increased by the reaction of excess anhydride groups, leading to an increased number of PA branches [39].

The most important rheological parameters determining the morphology development of immiscible blends are the viscosity and elasticity ratios of the components. The values of viscosity and elasticity ratio of the components, necessary to calculate their ratios, have been derived from the dynamic moduli by applying the Cox–Merz rule [41] for the pure polymers:

$$\eta^* = \eta_{ss}(\dot{\gamma} = \omega)$$

with η^* is the complex viscosity (Pa s), η_{ss}, steady shear viscosity (Pa s), $\dot{\gamma}$, steady shear rate, and ω, frequency.

As characteristic shear rate $\dot{\gamma}$ (in s^{-1}) in a twin-screw geometry the number of screw rotations per minute has been taken [40], i.e. 100 rpm (Table 2). Hence, the ratios are calculated from the dynamic data at 100 rad/s:

$$\text{viscosity ratio}: \; p = \frac{\eta^*\text{PA6}(100\ \text{rad/s})}{\eta^*\text{PS or } \eta^*(\text{PPE/PS})(100\ \text{rad/s})}$$

$$\text{elasticity ratio}: \; e = \frac{G'\text{PA6}(100\ \text{rad/s})}{G'\text{PS or } G'(\text{PPE/PS})(100\ \text{rad/s})}$$

The results are given in Table 3.

3.2. Reactive compatibilization of droplet/matrix blends

Before examining the effect of compatibilization on co-continuous blends, the efficiency of the compatibilization reaction was first investigated on droplet/matrix systems. For this purpose, two different series of blends were prepared. The first series consisted of a 75/25 PS/PA6 blend to which an increasing amount of SMA2 compatibilizer was added. In the second series, (PPE/PS) 50/50 (wt/wt) was used as the major component instead of PS. For both systems, two compatibilization strategies were applied, which differed by the way the SMA2 compatibilizer was mixed with the blend components. The efficiency of the compatibilization was expressed by the decrease in particle size as a function of the compatibilizer concentration.

All samples of the PS/PA6 75/25 blend series completely disintegrated when put in chloroform. Consequently, PA6 always formed the dispersed phase. As can be seen in Fig. 3, the size of the PA6 particles significantly decreases upon addition of the SMA2 compatibilizer. The torque, needed

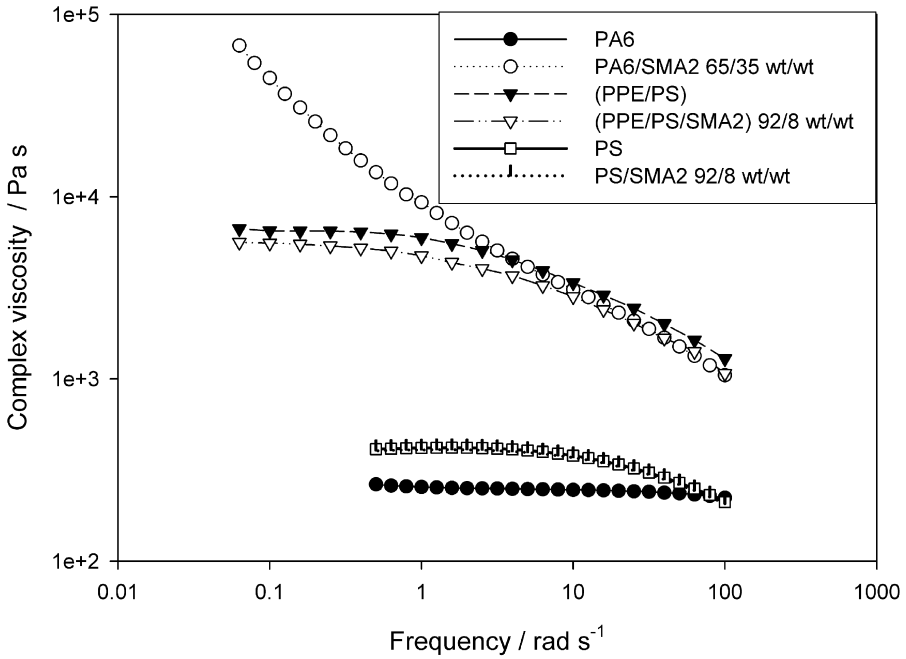

Fig. 1. Complex viscosity versus frequency for the blends and blend components extruded.

for melt mixing of the blends at a constant rotation rate of the screws in the extruder, did also rise with increasing amounts of compatibilizer, again indicating a rise in the blend viscosity.

In these ternary blends (PA6/X/SMA2), X = PS or (PPE/PS), the amino-end groups of PA6 will react with the anhydride groups of SMA2 during melt-mixing. This is a fast reaction; the direct reaction between amide groups of PA6 and anhydride groups is negligible compared to the reaction between the amino chain ends of PA6 and anhydride groups [39]. To be able to react, the SMA2 copolymer has to diffuse towards the interface of the blend phases. The graft copolymer that is formed at the interface will act as an emulsifier, which reduces the interfacial tension between the two phases. Furthermore, coalescence of dispersed droplets will be suppressed (presumably) via different mechanisms, like steric stabilization of the interface [42,43] or the presence of Marangoni stresses [44]. Both the phenomena result in a reduction in particle size with increasing interfacial reaction (Fig. 3). This figure also

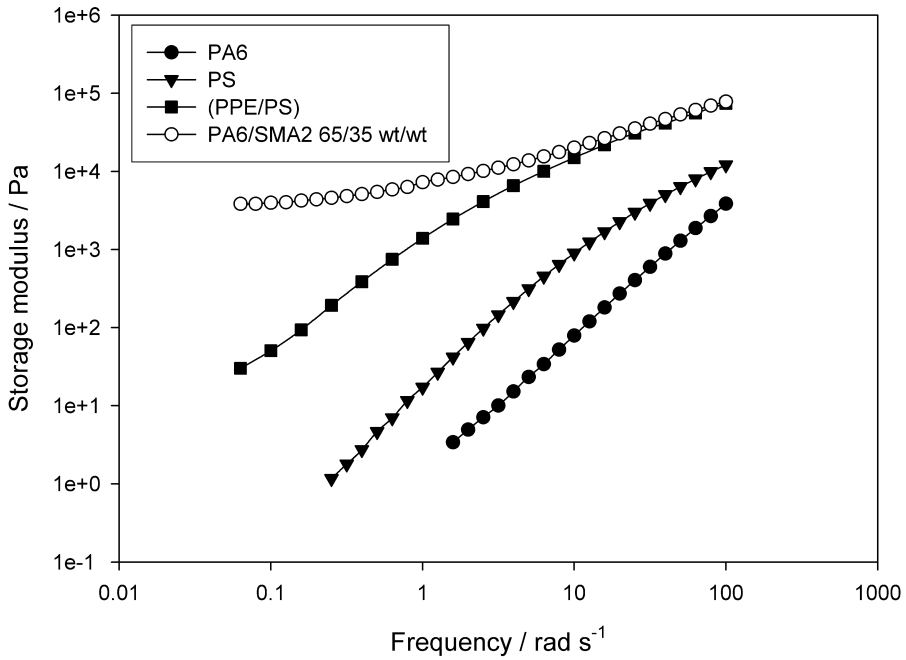

Fig. 2. Storage modulus versus frequency for the blend components and PA6/SMA2 65/35 blend.

Table 3
Rheological data of the blend components used

Sample	G' (100 rad/s) (Pa)	η^* (100 rad/s) (Pa s)	$\eta^*_{droplets}/\eta^*_{matrix} = p$ (PA6 minor phase)			$G'_{droplets}/G'_{matrix} = e$ (PA6 minor phase)		
			No SMA	Mixing method no. 1	Mixing method no. 2	No SMA	Mixing method no. 1	Mixing method no. 2
PS	12,100	211						
PS/SMA2 (92/8 wt/wt)	11,800	206	1.05	1.08	4.96	0.32	0.33	6.47
(PPE/PS)	74,000	1293						
(PPE/PS)/SMA2 (92/8 wt/wt)	64,700	1070	0.17	0.21	0.81	0.05	0.06	1.06
PA6	3900	222	–			–		
PA6/SMA2 (65/35 wt/wt)	78,300	1047	–			–		

shows for the PS/PA6 blend system, that the compatibilization is most efficient when SMA2 is premixed with PS prior to the final blending step.

Premixing PA6 with SMA2 (method no. 2) leads to a strong increase of the viscosity ratio as compared to the viscosity ratio of the uncompatibilized system, whereas the viscosity ratio η^*PA6/η^*(PS/SMA2) is almost identical to that of PA6/PS. As a result of this higher viscosity ratio the droplets of the dispersed phase break up less easily when SMA2 is premixed with PA6. Another explanation for the larger size of the dispersed phase in the (PA6/SMA2)/PS blend can be the fact that the in situ formation of PA6-*g*-SMA2 graft copolymer in the PA6 phase severely affects the diffusion of the compatibilizer towards the interface.

By substituting (PPE/PS) for PS in the blend, the PA6 particle size becomes much smaller, as can be seen by comparing Figs. 3 and 4. This can be attributed to the lower viscosity ratio in the former. A very broad particle size distribution develops in the uncompatibilized (PPE/PS)/PA6 75/25 blend; this will be discussed further in Section 3.3. For the compatibilized (PPE/PS)/PA6 blends, the difference between the two mixing methods for the SMA2 is less pronounced. This can be accounted for by the much higher viscosity of the PPE/PS phase as compared with pure PS. After compatibilization, the final sizes of the PA6 droplets are of the same order of magnitude in both blends. This confirms earlier observations that compatibilization reduces the effect of the viscosity/elasticity ratio on the blend morphology [34].

In summary, it can be stated that SMA2 is a very effective compatibilizer for both (PPE/PS)/PA6 and PS/PA6 blend systems. When SMA2 is premixed with the non-reactive phase, a very finely dispersed morphology of PA6 particles is obtained after adding about 5 wt% of the compatibilizer.

3.3. Reactive compatibilization of co-continuous blends

3.3.1. Formation of co-continuous structures during processing

In order to determine the co-continuous region for the two different blend systems the blend composition was varied systematically. However, premixing PS or PPE/PS with SMA2 proved to produce the best compatibilization, such mixtures were used systematically. They contained 8 wt% SMA2. Three different techniques were used to determine the structure: dissolution tests with two solvents, SEM visualization and quantitative extraction experiments.

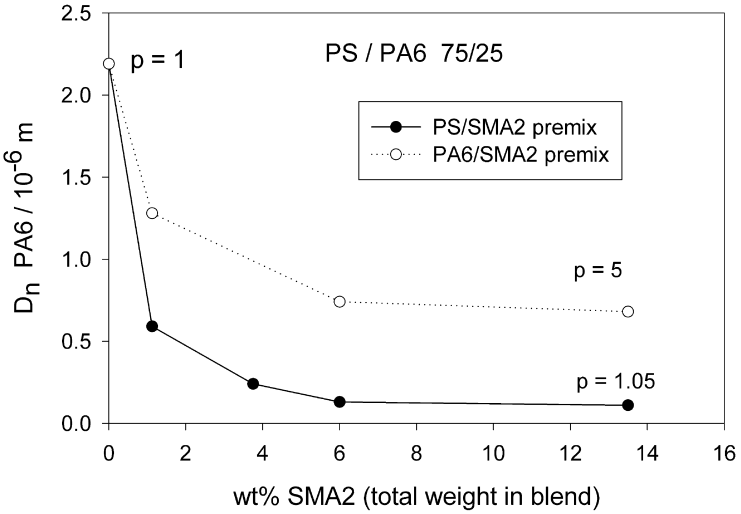

Fig. 3. Number average particle diameter of PA6 versus SMA2 concentration for PS/PA6 75/25 blend.

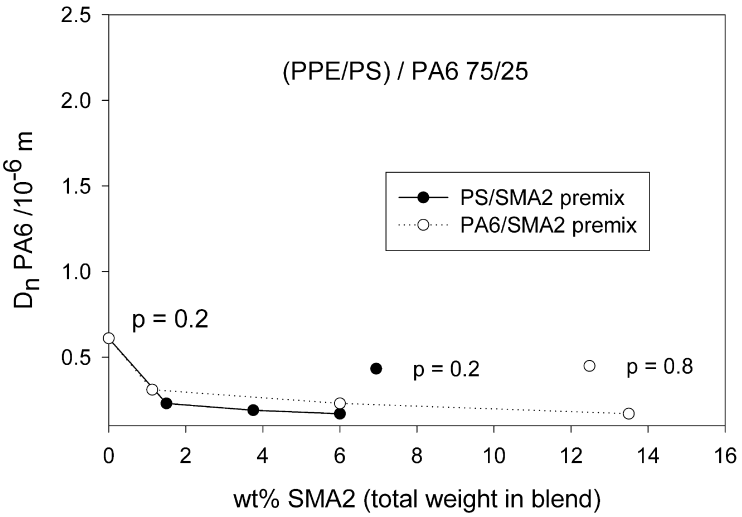

Fig. 4. Number average particle diameter of PA6 versus SMA2 concentration for (PPE/PS)/PA6 75/25 blend.

Fig. 5 shows the results of the dissolution tests; the concentration intervals for co-continuity, measured as discussed in Section 2.3, are schematically indicated for both PS/PA6 and (PPE/PS)/PA6 blends. In Fig. 6, the SEM micrographs for the PS/PA6 blend are presented as a function of the blend composition. These micrographs clearly show the transition from a droplet–matrix type of morphology to a co-continuous morphology with large, interpenetrating structures. SEM does not always provide the complete information about the blend phase morphology because of its 2D nature. Therefore, quantitative extraction experiments were performed as well. The percentage of PA6 phase that can be extracted from the sample is shown in Fig. 7 for the (PPE/PS)/PA6 and PS/PA6 blends.

The combined results of SEM, dissolution and extraction tests show that for both blend systems partial co-continuity is observed over a rather wide composition range. The region for full co-continuity for these blend systems

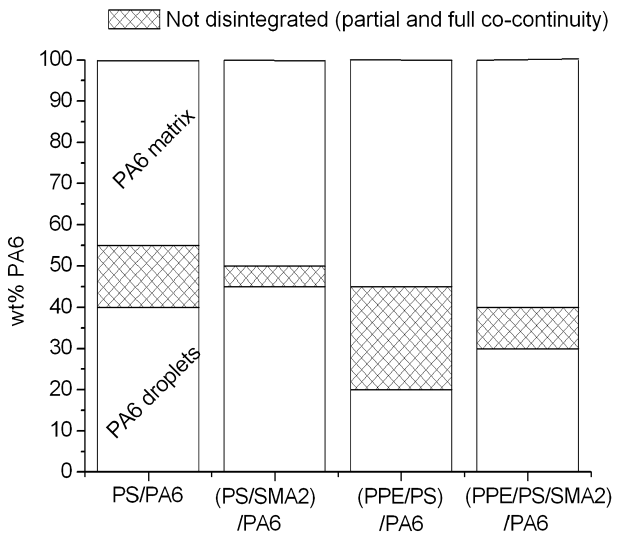

Fig. 5. Co-continuity intervals determined with dissolution tests on uncompatibilized and compatibilized blends.

characterized by 100% extraction, however, is relatively narrow, as can been seen from Fig. 7. A value for the interfacial tension of 8.5 mN/m was found for these blend systems using a Palierne analysis. A narrow region of full co-continuity is expected for such high interfacial tension blends, because the elongated threads will break up easily.

Figs. 5 and 7 show that in case of the (PPE/PS)/PA6 blends, the onset of co-continuity is shifted towards lower concentrations of PA6 than in PS/PA6, hence giving rise to a wider co-continuity interval. The concentration where PA6 becomes the matrix is also situated at a lower volume fraction. This can be seen from Fig. 7, where the composition for which disintegration of the blend in formic acid (a good solvent for PA6) took place, is indicated with arrows.

The shift of the phase inversion can be attributed to viscosity driven encapsulation of (PPE/PS); the less viscous component tends to encapsulate the more viscous one. As a result, the less viscous PA6 phase will have a tendency to form the matrix down to lower PA6 concentrations for the highly viscous (PPE/PS) phase. It should be emphasized that these co-continuous structures are not in equilibrium during flow inside the extruder. Especially for blends with a high interfacial tension a large amount of thread break-up is expected during processing. SEM micrographs taken from the plane parallel to the flow direction showed that the degree of anisotropy in the uncompatibilized co-continuous morphologies is relatively low and is similar to the co-continuous morphology obtained perpendicular to the flow direction (see Fig. 10(c)). This observation suggests that a large amount of thread break-up takes place during extrusion, which can probably be related to the transient, instead of stationary flow in twin-screw extrusion. The co-continuous morphology of this high interfacial tension blend will thus only be maintained by recombination and coalescence processes.

Scott et al. [45] and Sundararaj et al. [46] thoroughly

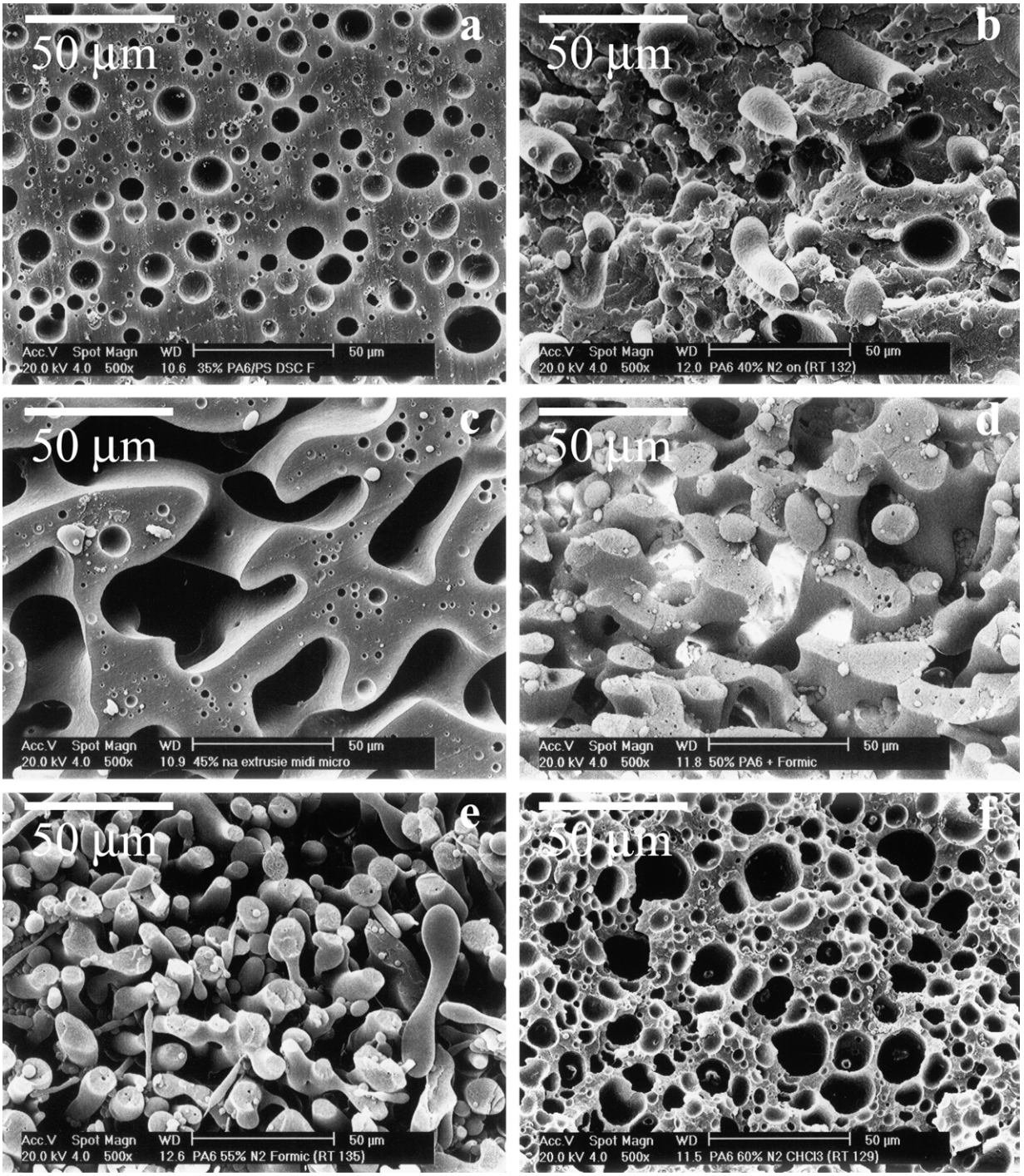

Fig. 6. SEM photographs of different PS/PA6 blend components (a) 35% PA6, (b) 40% PA6, (c) 45% PA6, (d) 50% PA6, (e) 55% PA6, (f) 60% PA6.

investigated phase inversion during the processing of immiscible blends at various temperatures. Such an inversion occurred when the major component had a higher melting or softening temperature than the minor component. When the minor component melts or softens first and becomes the continuous phase, it encapsulates the dispersed solid pellets of the major component. Once the major component melts also, the mixture undergoes a phase inversion and the major component will become the continuous phase. It was observed that this phase inversion process could be severely affected by the softening/melting phenomena of the blend components. Only when a significant amount of the higher melting component had softened, gradual phase inversion could proceed. Hence, it can be anticipated that a higher melt viscosity and a higher glass transition temperature of the major component will

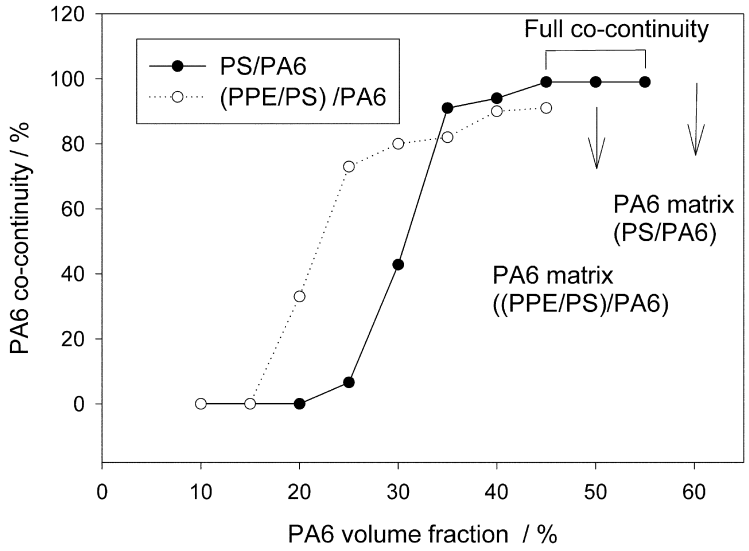

Fig. 7. PA6 co-continuity for PS/PA6 and (PPE/PS)/PA6 blends, as determined with extraction experiments (arrows indicate composition of disintegration in formic acid (solvent for PA6)).

increase the time required to reach a steady state morphology. These observations suggest that substituting PS by (PPE/PS), which has a much higher T_g and viscosity, can severely affect the time required to reach a steady state morphology during extrusion. This could result in a wider co-continuity interval for the (PPE/PS)/PA6 blend after extrusion. Experiments at different extrusion times from 3 up to 30 min for (PPE/PS)/PA6 80/20 and 75/25 blends, however, displayed no change in the co-continuity interval. Sundararaj et al. [46], suggested that the melting order of the components might cause a metastable co-continuous morphology even at long mixing times for blends with a low concentration (down to 5 wt%) of one of the phases.

Another clear difference between the two blend series is that, for the (PPE/PS)/PA6 blends, the maximum amount of extracted PA6 is about 90%, whereas for the PS/PA6 blends almost 100% extraction is reached. Hence, a fully co-continuous phase network for PA6 is never obtained when using (PPE/PS). With SEM quite complex co-continuous morphologies could be observed for the (PPE/PS)/PA6 blends, especially at lower PA6 volume fractions. An example of such morphology can be seen in Fig. 8. This SEM picture shows the phase morphology for a (PPE/PS)/PA6 70/30 blend where the PA6 phase was etched away with formic acid. The percentage of co-continuity for this blend is about 80%. It can be seen that a considerable amount of the PA6 phase is not a part of the co-continuous network, but present as small particles inside the (PPE/PS) phase. The existence of these small PA6 particles could also be detected from DSC experiments via fractionated crystallization [47].

The formation of similar morphologies has also been reported for several other blend systems that were mixed in the phase inversion region [48–50]. Berger et al. [49] assumed that sub-inclusion formation in PET/PA6 blends was affected by the elasticity difference between the two phases. In one case, a high viscosity ratio was considered to be the cause of such a composite phase morphology. Favis et al. [50], however, also found considerable sub-inclusion formation in PS/PE and PC/PP blends, which had a relatively low elasticity and viscosity ratio.

The mechanism for phase inversion during processing proposed as by Sundararaj et al. [46] shows that during the phase inversion process, small particles of the major phase may be trapped inside the minor phase. The presence of many sub-inclusions in the blends containing (PPE/PS) with high T_g and high viscosity, may indicate that the chance for trapping particles will be larger for slowly developing phase morphologies.

Summarizing, the morphological data for the PS/PA6 and (PPE/PS)/PA6 blends presented here can be explained by a difference in viscosity ratio leading to a shift in the

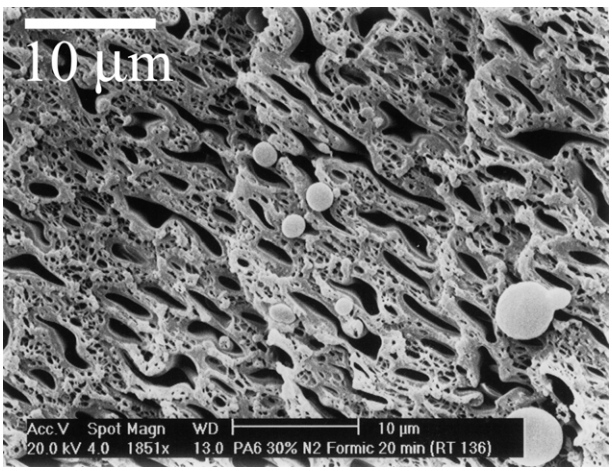

Fig. 8. SEM photograph of a (PPE/PS)/PA6 70/30 blend after dissolution of PA6 using formic acid (black in graph) showing small sub-inclusions.

phase inversion concentration as well as in the onset of co-continuity towards lower PA6 concentrations. No clear effect of the change in elasticity ratio for these blend systems has been found for the present systems, indicating the dominating effect of the viscosity over the elasticity. The wide range of partial co-continuity for slowly developing phase morphologies is supposed to be related to the difference in softening or melting behavior of the blend components inside the extruder. It is suggested that the formation of complex composite blend morphologies can be best understood as a result of the complex phase inversion process during processing (mostly in the initial stages of mixing).

In Fig. 9 the SEM micrographs for the PS/PA6 blends after reactive compatibilization with SMA2 are displayed for several blend compositions. Morphological data before and after compatibilization are presented in Table 4 (after applying DSC heating treatment). Compatibilization has a significant effect on the formation of co-continuous structures. The dissolution results given in Fig. 5 show that the width of the composition interval for (full) co-continuity is reduced for both blend series after compatibilization. The compatibilized PS/PA6 blends with 40 and 55% PA6 show a droplet–matrix type of morphology, as can be seen in Fig. 9(b) and (e) (note the difference in magnification). These blends disintegrate into one of the selective solvents. For the other two compositions (45 and 50% PA6), the domain size of the co-continuous phase is significantly reduced upon reactive compatibilization with SMA2, leading to a strong increase in interfacial area. The co-continuous structure remains, however, intact.

In Fig. 10(a) the SEM photograph of the (PS/SMA2)/PA6 (51/4)/45 blend is shown taken parallel to the flow direction. The degree of anisotropy after extrusion for these compatibilized blends is increased in the direction parallel to the flow direction (Fig. 10(b)). A substantial increase in the degree of elongation of the co-continuous threads can be observed in comparison with the uncompatibilized co-continuous blends (Fig. 10(c) and (d)). This can be attributed to the decreased interfacial tension after compatibilization. A lower interfacial tension is expected to entail larger deformations of the threads and to enhance their stability. Jansseune et al. [51] found that highly concentrated blend mixtures with a moderate interfacial tension can display a high amount of fibrillar structures under steady shear flow. These structures could not be characterized as co-continuous because no real network was formed; after stopping the shear flow, the fibrils broke up into droplets. The degree of anisotropy as obtained here in the compatibilized blends, is, however, far less than that observed by Jansseune et al. [51], the morphologies obtained can clearly be characterized as co-continuous. This can probably again be explained by the complex transient flow during twin-screw extrusion, compared to the stationary flow in the experiments of Jansseune et al. [51].

3.3.2. Stability of the co-continuous morphology during annealing

In the next series of experiments the stability of the co-continuous morphologies during annealing under quiescent conditions was investigated. The extruded polymer strands were heated in a Mettler FP90 oven under constant N_2-flow. Two different heating treatments were used. The first heating treatment consisted of the thermal program typically used in dynamic crystallization experiments with DSC. In the second treatment, the samples were annealed for 1 h at 260 °C in the oven. In Fig. 11, the concentration intervals for the PS/PA6 and (PPE/PS)/PA6 blends are shown in which no disintegration took place in either of the dissolution solvents after annealing for 1 h. This figure can be compared with the results for similar unannealed samples (see Fig. 5).

For the PS/PA6 system, the 60/40 blend composition breaks-up very rapidly and develops a droplet–matrix morphology with PA6 as the dispersed phase. Even by applying the DSC thermal program all co-continuity was lost and a broad size distribution of PA6 particles resulted (see Table 4). The 55/45 blend composition did, however, not show break-up under quiescent conditions, not even when the sample was annealed for 2 h. As can be seen in Fig. 12 the co-continuous morphology showed strong phase coarsening as a result of the annealing treatment but did not break-up into a droplet–matrix structure; the co-continuous network remained intact. The same observations were made on the 50/50 and 45/55 blend compositions.

For the (PPE/PS)/PA6 blend series all blend compositions below 45% PA6 did break up into a droplet–matrix morphology with PA6 as the dispersed phase. The blend compositions below 40% PA6 did already break up after the DSC thermal program, whereas the 40% PA6 blend composition only broke up after 1 h of annealing. Only the 55/45 blend composition remained co-continuous after both heating treatments, but it showed strong phase coarsening. The droplet–matrix morphologies formed after break-up of the co-continuous structure had a very broad particle size distribution of PA6 particles. Typical bimodal distributions were formed, consisting of a population of large particles of about 10–30 μm and a second population of very small particles of about 0.3 μm (see Table 4).

The effect of the viscosity or elasticity ratio on the quiescent annealing behaviour is not easily determined from the above experiments. It is, however, remarkable that almost all (PPE/PS)/PA6 blend compositions evolved into a droplet/matrix morphology, whereas most of the PS/PA6 blends only showed strong phase coarsening. These observations are similar to those of Veenstra et al. [52] and Willemse et al. [53]. These authors reported that above a certain concentration of the dispersed phase the morphology did not completely broke up, but only showed phase coarsening of the co-continuous domains. Willemse [54] proposed a relation for the critical blend composition wherefore the co-continuous network was stable, based on

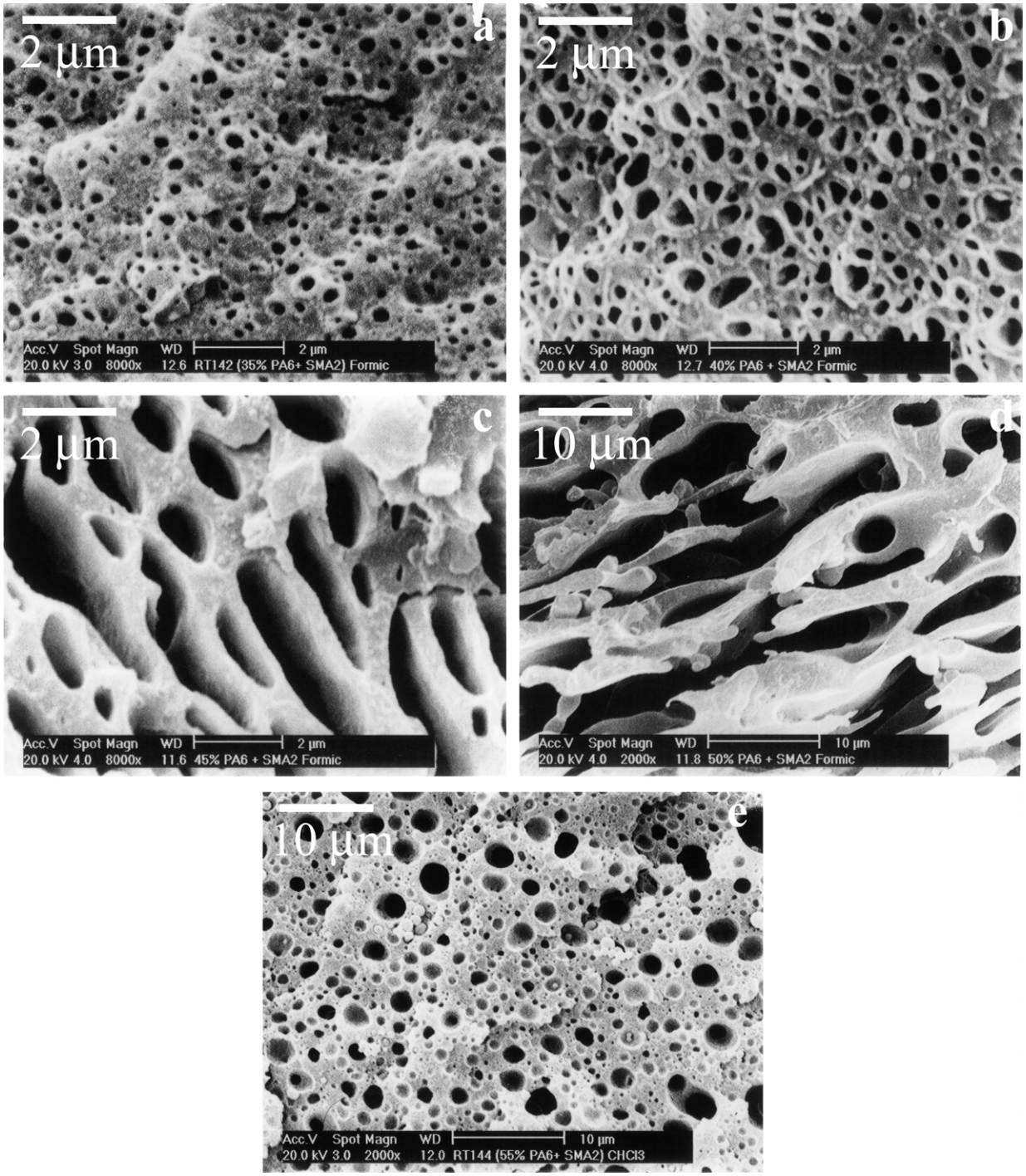

Fig. 9. SEM photographs of different PS/PA6 blend components compatibilized with SMA2, (a) 35% PA6, (b) 40% PA6, (c) 45% PA6, (d) 50% PA6, (e) 55% PA6.

the critical aspect ratio of threads and the geometrical requirements of a co-continuous morphology. Above the critical concentration, depending only on the viscosity ratio, no break up occurred, but the threads retracted, leading to a coarsened co-continuous structure.

Compatibilization with SMA2 has a significant effect on the stability of the co-continuous morphologies. A comparison of Figs. 5 and 12 shows that it effectively stabilizes the co-continuous blend morphology during a quiescent thermal treatment. It was also found that, upon annealing during 15 min at 260 °C, the degree of anisotropy in the longitudinal direction decreased rapidly. The phase

Table 4
Morphological parameters determined from image analysis and disintegration experiments for uncompatibilized and SMA2 compatibilized PS/PA6 and (PPE/PS)/PA6 blend compositions

PA6 (wt%)	PS/PA6		(PS/SMA2[a])/PA6		(PPE/PS)/PA6		(PPE/PS/SMA2[a])/PA6	
	$D_{n,PA6}$ (μm)	(D_v/D_n)	$D_{n,PA6}$ (μm)	(D_v/D_n)	$D_{n,PA6}$ (μm)	(D_v/D_n)	$D_{n,PA6}$ (μm)	(D_v/D_n)
15	1.4	1.6	–	–	0.35	3.1	0.09	1.7
20	1.8	1.5	–	–	0.57[b]	9.3	0.13	1.6
25	2.1	2.4	0.11	1.5	0.61[b]	12.4	0.17	1.8
30	2.8	2.7	0.15	1.4	4.6[c]	3.9	Co-cont.	–
35	3.7	2.6	0.19	1.6	5.1[c]	4.7	Co-cont.	–
40	7.0[c]	4.8	0.29	1.9	Co-cont.	–	Co-cont.	–
45	Co-cont.	–	Co-cont.	–	Co-cont.	–	PA6 matrix	–
50	Co-cont.	–	Co-cont.	–	PA6 matrix	–	PA6 matrix	–
55	Co-cont.	–	PA6 matrix	–	PA6 matrix	–	PA6 matrix	–

[a] Morphological data for initial PS/SMA2 and (PPE/PS)/SMA2 compositions of 92/8 (wt/wt), except (PPE/PS/SMA2)/PA6 80/20 and 85/15, with (PPE/PS/SMA2) 95/5 premixture (all method no. 1).
[b] Broad, bimodal particle size distribution due to break-up of co-continuous structure.
[c] Broad particle size distribution due to break-up of initial co-continuous structure.

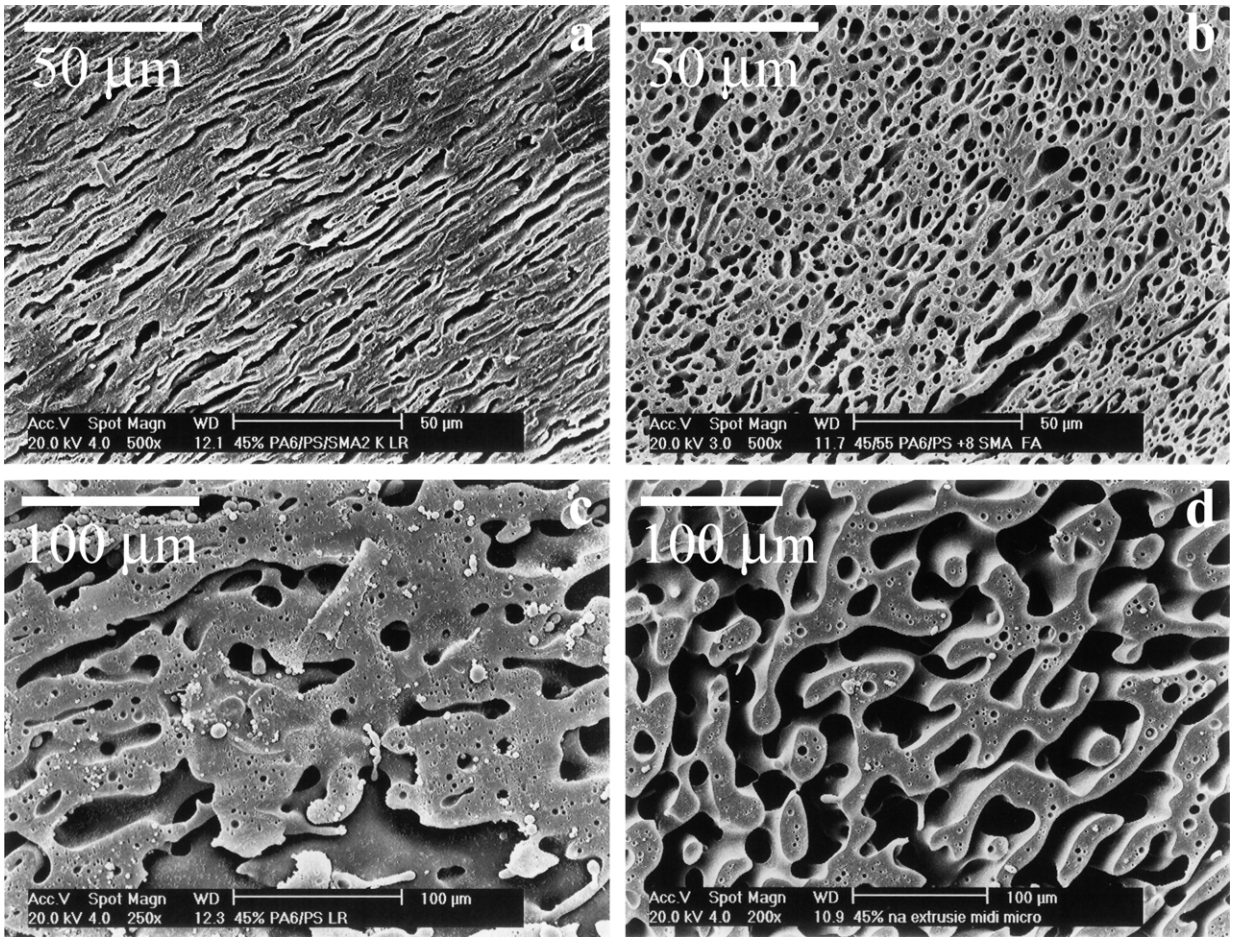

Fig. 10. SEM photographs of co-continuous phase morphologies, (a) (PS/SMA2)/PA6 (51/4)/45 blend, parallel to the flow direction, (b) perpendicular to the flow direction, (c) PS/PA6 55/45 blend, parallel to the flow direction, (d) perpendicular to the flow direction.

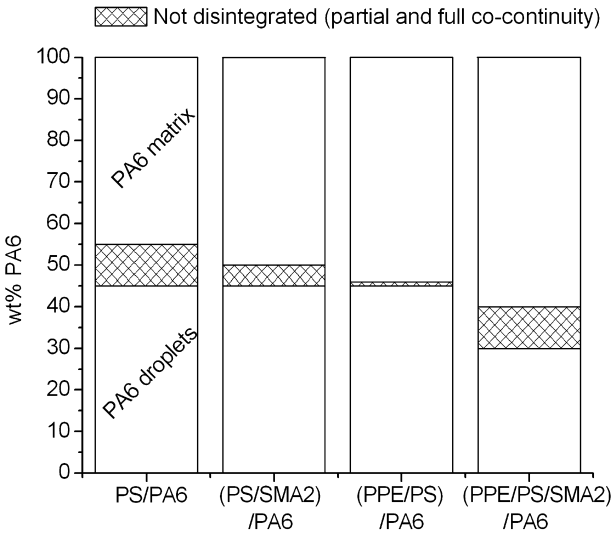

Fig. 11. Co-continuity intervals determined with dissolution tests on uncompatibilized and compatibilized blends after annealing for 1 h at 260 °C.

coarsening for the blends is limited after compatibilization, as can be clearly seen from Fig. 13 where the morphology is shown for the (51/4)/45(PS/SMA2)PA6 blend composition before and after the annealing treatment. Addition of SMA2 compatibilizer reduces the tendency for phase coarsening via lowering of the interfacial tension, because the coalescence ability of particles under quiescent conditions is expected to be low.

3.3.3. Discussion: comparison of the effect of the compatibilizer in quiescent and flow conditions

The results presented above clearly show the opposite effects of the SMA2 compatibilizer on the co-continuous phase morphology development. Under flow conditions, when the structures are formed inside the extruder, SMA2 seems to decrease the network stability, whereas under quiescent conditions SMA2 clearly enhances the stability. It is therefore very important to clearly differentiate between quiescent conditions and flow conditions in the extruder.

Under quiescent conditions a stable co-continuous morphology can be preserved when break-up and retraction processes are sufficiently suppressed. A lower interfacial tension reduces the driving force for these processes. When, however, flow is applied, as during processing, a dynamic equilibrium between break-up processes and coalescence or recombination phenomena is a prerequisite for maintaining a co-continuous network. Strong flow conditions are known to favor break-up and coalescence processes. Under flow, a lower interfacial tension does not automatically ensure a more stable co-continuous system. When the interfacial tension is lower the domains are more easily deformed into long, elongated threads although their stability is enhanced. This was also shown in this paper from SEM micrographs taken parallel to the flow direction. Depending on the interfacial tension, blend composition and flow, these threads will either break-up or remain elongated. A low interfacial tension has been shown to favor a wide co-continuity interval [11,14] but it can be anticipated that break-up also occurs for these blends, because thread deformation in these blends takes place very easily. The type of flow can have dramatic effects on the thread formation, leading to strongly elongated threads in stationary flow, which usually are not obtained to the same extent in transient flow [51].

For immiscible blends, with a large interfacial tension, such as PS/PA6, the break-up and retraction processes occur rapidly. Hence, recombination and coalescence during flow of the broken threads are essential to preserve the co-continuous network structure in these blends. From the morphological data on the reactively compatibilized co-continuous blends, it is clear that these coalescence and recombination phenomena are effectively suppressed by the graft copolymer that has been formed at the interface between the two blend phases. As a result, a smaller width of the co-continuity interval can be expected for the

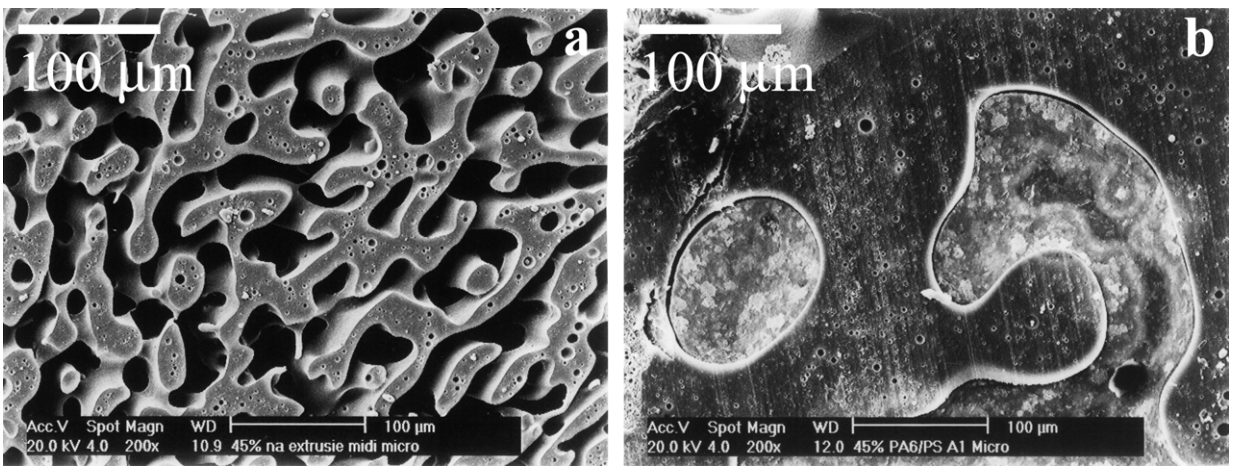

Fig. 12. SEM photographs of PS/PA6 55/45 blend (a) directly after extrusion, (b) after annealing for 1 h at 260 °C.

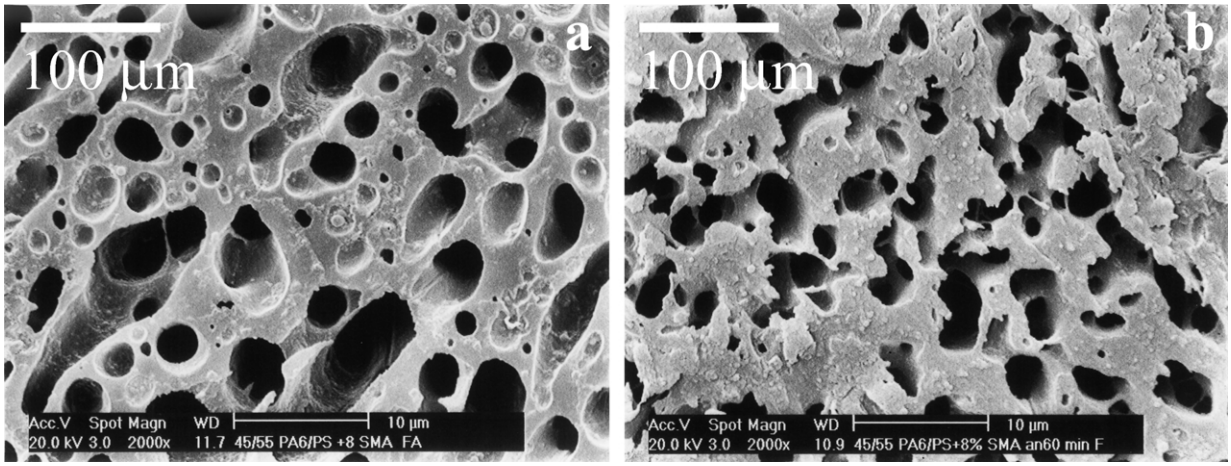

Fig. 13. SEM photographs of (PS/SMA2)/PA6 (51/4)/45 blend (a) directly after extrusion, (b) after annealing for 1 h at 260 °C.

compatibilized blends although the interfacial tension is lowered.

4. Conclusions

In this paper, it was demonstrated that co-continuous phase morphologies can be obtained over a relative broad composition range via melt-extrusion of two immiscible polymers.

The range of full co-continuity as derived from extraction experiments, was narrow as expected for blends with a high interfacial tension. Using a combination of SEM and extraction techniques, it has been shown that the shifts in the phase inversion and in the co-continuity onset are related to a change in viscosity ratio. It is argued that the melting order of the components inside the extruder can result in a broadening of the observed co-continuity interval and in the formation of complex composite morphologies in slowly developing phase morphologies.

The uncompatibilized co-continuous morphologies are very unstable under quiescent annealing conditions and do break-up or show strong phase coarsening depending on the blend composition. Although the quiescent stability of the threads improved upon compatibilization because of the lower resulting interfacial tension, the decreased possibility for recombination and coalescence during flow reduced the co-continuity region for the compatibilized blends. It can thus be concluded that during flow a dynamic equilibrium between break-up and recombination phenomena is very important to maintain the network structure after the initial network formation. These results are in agreement with the general predictions of Li et al. [27] for blends with a high interfacial tension. As a consequence, the effect of compatibilization on the co-continuity region cannot by predicted a priori, but depends critically on the interfacial tension of the blend system considered and the amount and type of flow applied during processing of the co-continuous blends.

Acknowledgements

The authors are indebted to the Fund for Scientific Research Flanders (FWO-Vlaanderen) as well as to the Research Fund KULeuven (GOA 98/06 project) for financial support.

References

[1] Avgeropoulos GN, Weissert FC, Biddison PH, Bohm GGA. Rubber Chem Technol 1976;49:93.
[2] Paul DR, Barlow JW. Macromol Sci, Rev Macromol Chem 1980;C18:109.
[3] Jordhamo GM, Manson JA, Sperling LH. Polym Engng Sci 1986;26:507.
[4] Miles IS, Zurek A. Polym Engng Sci 1988;28:796.
[5] Metelkin VI, Blekht VS, Kolloid Z. 1984;46:476
[6] Utracki LA. J Rheol 1991;35:1615.
[7] De Roover B, Devaux J, Legras R. J Polym Sci, Part A: Polym Chem 1997;35:917.
[8] Lyngaae-Jorgensen J, Utracki LA. Makromol Chem, Makromol Symp 1991;48/49:189.
[9] Willemse RC, Posthuma de Boer A, van Dam J, Gotsis AD. Polymer 1998;39:5879.
[10] Willemse RC, Posthuma de Boer A, van Dam J, Gotsis AD. Polymer 1999;40:827.
[11] Veenstra H, van Dam J, Posthuma de Boer A. Polymer 1999;40:1119.
[12] Veenstra H, Norder B, van Dam J, Posthuma de Boer A. Polymer 1999;40:5223.
[13] He J, Bu W, Zeng J. Polymer 1997;38:6347.
[14] Verhoogt H, van Dam J, Posthuma de Boer A. Adv Chem Ser 1994;239:333.
[15] Dedecker K, Groeninckx G. Polymer 1998;39:4993.
[16] Favis BD, Chalifoux JP. Polymer 1988;29:1761.
[17] Mekhilef N, Verhoogt H. Polymer 1996;37:4069.
[18] Kitayama N, Keskkula H, Paul DR. Polymer 2000;41:8041.
[19] Li JM, Favis BD. Macromolecules 2002;35:2005.

[20] Chuai CZ, Almdal K, Lyngaae-Jorgensen J. Polymer 2003;44:481.
[21] Steinmann S, Gronski W, Friedrich C. Polymer 2001;42:6619.
[22] Bourry D, Favis BD. J Polym Sci, Part B: Polym Phys 1998;36:1889.
[23] Van Oene H. J Colloid Interf Sci 1972;40:448.
[24] Scott CE, Macosko CW. Polymer 1995;36:461.
[25] Sundararaj U, Macosko CW, Rolando RJ, Chan HT. Polym Engng Sci 1992;32:1814.
[26] Luciani A, Jarrin J. Polym Engng Sci 1996;36:1619.
[27] Li JM, Ma PL, Favis BD. Macromolecules 2002;35:2005.
[28] Quintens D, Groeninckx G, Guest M, Aerts L. Polym Engng Sci 1990; 30:1484.
[29] Harrats C, Blacher S, Fayt R, Jérôme R, Teyssié P. J Polym Sci, Part B: Polym Phys 1995;33:801.
[30] Mekhilef N, Favis BD, Carreau PJ. J Polym Sci, Part B: Polym Phys 1997;35:293.
[31] Gergen WP, Lutz RG, Davison S. In: Legge NR, editor. Thermoplastic elastomers. A comprehensive review. Munich: Hanser; 1986. p. 507. Chapter 14.
[32] Chapleau N, Favis BD, Carreau PJ. J Polym Sci, Part B: Polym Phys 1998;36:1947.
[33] Elemans PHM, Janssen JMH, Meijer HEH. J Rheol 1990;34:1311.
[34] Willis JM, Caldas V, Favis BD. J Mater Sci 1991;26:4742.
[35] Everaert V, Groeninckx G, Pionteck J, Favis BD, Aerts L, Moldenaers P, Mewis J. Polymer 2000;41:1011.
[36] Fried JR, Hanna GA. Polym Engng Sci 1982;22:705.
[37] Witteler H, Leiser G, Drosher M. Makromol Chem Rapid Commun 1993;14:401.
[38] Vankan R, Degée P, Jérôme R, Teyssié P. Polym Bull 1994;33:221.
[39] Van Duin M, Aussems M, Borggreve RJM. J Polym Sci, Part A: Polym Chem 1998;36:179.
[40] Macosko CW. Rheology, principles, measurements, and applications. Weinheim: VCH Publishers; 1994. Chapter 4.
[41] Wu S. Polym Engng Sci 1987;27:335.
[42] Majumdar B, Keskkula H, Paul DR. Polymer 1994;35:1386.
[43] Wildes G, Keskkula H, Paul DR. Polymer 1999;40:5609.
[44] Van Puyvelde P, Velankar S, Moldenaers P. Curr Opin Colloid Interf Sci 2001;6:457.
[45] Scott CE, Young SK. Proceedings of the SPE Retec Symposium on Polymer Alloys and Blends, Boucherville, Canada, October; 1995. p. 338.
[46] Sundararaj U, Macosko CW, Shih CK. Polym Engng Sci 1996;36: 1769.
[47] Tol RT, Mathot VBF, Groeninckx G. 2004 in press.
[48] Everaert V, Groeninckx G. Polymer 1999;40:6627.
[49] Berger W, Kammer HW, Kummerlöwe C. Makromol Chem Suppl 1984;8:101.
[50] Favis BD, Lavallee C, Derdouri A. J Mater Sci 1992;27:4211.
[51] Jansseune T, Moldenaers P, Mewis J. J. Rheol. 2003;47(4):829.
[52] Veenstra H, van Dam J, Posthuma de Boer A. Polymer 2000;41:3037.
[53] Willemse RC, Ramaker EJJ, van Dam J. Posthuma de Boer A. Polym Engng Sci 1999;39:1717.
[54] Willemse RC. PhD Thesis. TUDelft, The Netherlands; 1998.